iScience

CellPress
OPEN ACCESS

Article

Multiplexed CRISPR gene editing in primary human islet cells with Cas9 ribonucleoprotein

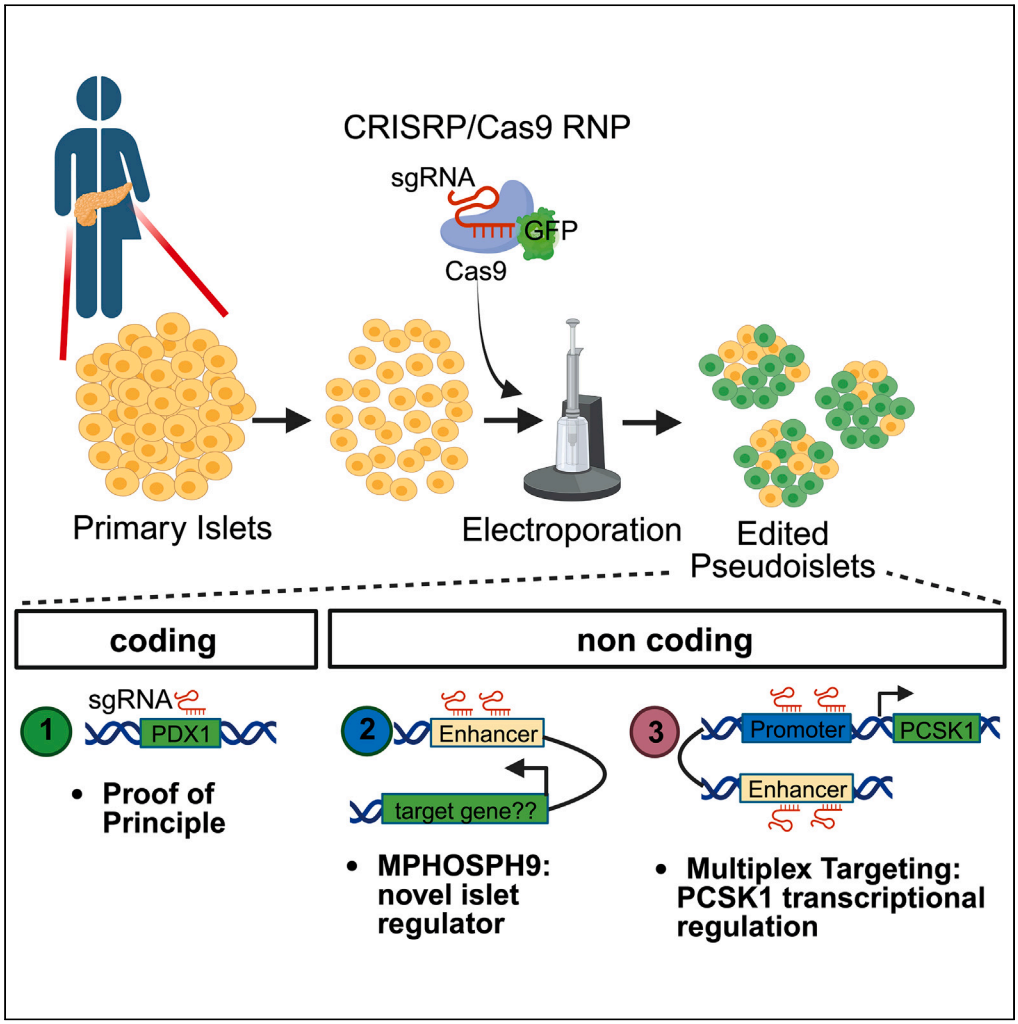

Romina J. Bevacqua, Weichen Zhao, Emilio Merheb, Seung Hyun Kim, Alexander Marson, Anna L. Gloyn, Seung K. Kim

romina.bevacqua@mssm.edu (R.J.B.)
seungkim@stanford.edu (S.K.K.)

Highlights

CRISPR/Cas9 RNP editing of coding and non-coding DNA in primary human islet cells

Identified *MPHOSPH9* as an unsuspected regulator of β cell insulin secretion

CRISPR/Cas9 RNP allows multiplexed targeting of *PCSK1 cis*-regulatory elements

Identified *cis*-regulatory elements regulating glucose-dependent *PCSK1* expression

Bevacqua et al., iScience *27*, 108693
January 19, 2024
https://doi.org/10.1016/j.isci.2023.108693

iScience

CellPress
OPEN ACCESS

Article

Multiplexed CRISPR gene editing in primary human islet cells with Cas9 ribonucleoprotein

Romina J. Bevacqua,[1,2,*] Weichen Zhao,[1] Emilio Merheb,[2] Seung Hyun Kim,[1] Alexander Marson,[3,4,5,6] Anna L. Gloyn,[7,9] and Seung K. Kim[1,8,9,10,11,*]

SUMMARY

Successful genome editing in primary human islets could reveal features of the genetic regulatory landscape underlying β cell function and diabetes risk. Here, we describe a CRISPR-based strategy to interrogate functions of predicted regulatory DNA elements using electroporation of a complex of Cas9 ribonucleoprotein (Cas9 RNP) and guide RNAs into primary human islet cells. We successfully targeted coding regions including the *PDX1* exon 1, and non-coding DNA linked to diabetes susceptibility. CRISPR-Cas9 RNP approaches revealed genetic targets of regulation by DNA elements containing candidate diabetes risk SNPs, including an *in vivo* enhancer of the *MPHOSPH9* gene. CRISPR-Cas9 RNP multiplexed targeting of two *cis*-regulatory elements linked to diabetes risk in *PCSK1*, which encodes an endoprotease crucial for Insulin processing, also demonstrated efficient simultaneous editing of *PCSK1* regulatory elements, resulting in impaired β cell *PCSK1* regulation and Insulin secretion. Multiplex CRISPR-Cas9 RNP provides powerful approaches to investigate and elucidate human islet cell gene regulation in health and diabetes.

INTRODUCTION

Impaired pancreatic islet function underlies nearly all forms of diabetes mellitus, including type 1 (T1D) and type 2 diabetes (T2D).[1] Islets comprise clustered hormone-producing cells, called β, α, δ, ε, and PP cells, that govern glucose and other key regulators of metabolism. Genetic and acquired risks are thought to impact islet function and promote diabetes development.[2–4] In both T1D and T2D, genetic risk has been linked to non-coding DNA variants, with a preponderance of these located in active islet gene regulatory regions called enhancers.[5,6] Recent studies show that islet enhancers change their chromatin accessibility during lineage progression and maturation,[7] upon glucose stimulation,[8] and upon cytokine exposure.[9] However, challenges in studying human islet enhancers, promoters, and other *cis*-regulatory elements have limited our understanding of how these are mechanistically linked to diabetes risk.[10,11]

Attempts to study gene regulation in primary human islet cells face multiple hurdles including: (1) the relatively small number of islet cells per pancreas, (2) their lack of expansion—islet cells are largely non-dividing, (3) the characteristic clustering of islet cells that limits efficient genetic targeting, (4) the harsh nucleolytic environment of the exocrine pancreas surrounding native islets, and (5) a lack of methods to target or edit non-coding DNA elements in primary islets. To address these technical gaps, we innovated methods for genetic modification of primary human islet cells using CRISPR/Cas9-based approaches. We previously showed efficient gene editing of primary human islet cells using lentiviruses simultaneously encoding Cas9, a single-stranded guide RNA (sgRNA), and GFP.[12] This system combined with our transient dispersion of primary islet cells followed by reaggregation into organoids called "pseudoislets" (reviewed in Friedlander et al.[13]) allowed efficient gene editing of both coding and non-coding genomic regions in primary human islet cells. However, lentivirus-based CRISPR/Cas9 targeting (hereafter, lentiCRISPR) is relatively labor intensive, requiring cloning of candidate sgRNAs, followed by production of virus in sufficient titers and then isolation of infected cells for analysis. These multiple steps reduce yields for cell or nucleic acid-based assays, limit ease of scalability or genetic screens, and result in lentiviral integration in the genome of the targeted cell.

Electroporation of Cas9 ribonucleoprotein preloaded with sgRNAs (CRISPR/Cas9 RNP) has been successfully used for gene editing in challenging cellular targets, including embryonic stem cells, induced pluripotent stem cells, tissue stem cells, and T lymphocytes,[14–17] but has not

[1]Department of Developmental Biology, Stanford University School of Medicine, Stanford, CA 94305, USA
[2]Diabetes, Obesity and Metabolism Institute (DOMI), Icahn School of Medicine at Mount Sinai, New York, NY 10029, USA
[3]Gladstone-UCSF Institute of Genomic Immunology and Northern California JDRF Center of Excellence, University of California at San Francisco, San Francisco, CA 94158, USA
[4]Department of Medicine, University of California, San Francisco, San Francisco, CA 94143, USA
[5]Diabetes Center, University of California, San Francisco, San Francisco, CA 94143, USA
[6]Department of Microbiology and Immunology, University of California, San Francisco, San Francisco, CA 94143, USA
[7]Department of Pediatrics (Endocrinology) and of Genetics, Stanford University School of Medicine, Stanford, CA 94305, USA
[8]Departments of Medicine and of Pediatrics, Stanford University School of Medicine, Stanford, CA 94305, USA
[9]Stanford Diabetes Research Center, Stanford University School of Medicine, Stanford, CA 94305, USA
[10]Northern California JDRF Center of Excellence, Stanford University School of Medicine, Stanford, CA 94305, USA
[11]Lead contact
*Correspondence: romina.bevacqua@mssm.edu (R.J.B.), seungkim@stanford.edu (S.K.K.)
https://doi.org/10.1016/j.isci.2023.108693

previously been reported for adult human islet cells, which are post-mitotic. Direct delivery of CRISPR/Cas9 RNP complexes can bypass the requirement for transcription and translation, allowing rapid and efficient genome editing. In contrast to lentiCRISPR approaches, CRISPR/Cas9 RNP does not involve integration of sequences encoding *Cas9 or sgRNA* into the genome. Thus, the only genomic modification introduced is the specific gene edit. The short half-life of the CRISPR/Cas9 RNP complex reduces off-target effects, and the chance for insertional mutagenesis, and immune responses.[18,19] The simplicity of this approach can also enable simultaneous ("multiplex") editing of multiple genetic targets[16] like promoters and enhancers. Here, we investigated use of CRISPR/Cas9 RNP-based multiplex targeting of *cis*-regulatory elements in primary human islet cells.

RESULTS

CRISPR/Cas9 RNP electroporation to target PDX1 in primary human islet cells

To innovate CRISPR gene editing in primary human islet cells, we electroporated Cas9 protein fused with GFP with sgRNAs into dispersed human islet cells (Figure 1A: STAR methods). Afterward, islet cells reaggregated to form pseudoislets that were assayed after 6 days, as we previously reported using the lentiCRISPR approach.[12]

To optimize CRISPR/Cas9 RNP electroporation, we systematically varied voltage, and concentration of Cas9 RNP "preloaded" with sgRNA specific for exon 1 of *PDX1* (Figure 1B; Figure S1A, STAR methods) and then visualized Cas9-GFP fluorescence one day after electroporation (Figure 1C). To assess the toxicity of our approach, we evaluated cell viability following electroporation with CRISPR/Cas9 RNP and 2 control sgRNAs and detected an average 70% live cells 5 days following electroporation, as compared to isochronic non-electroporated pseudoislets (95% live cells; Figures S1B–S1E, STAR methods). Following 6 days of *in vitro* pseudoislet culture, we extracted genomic DNA and performed next-generation sequencing of the indexed amplicons (STAR methods). Insertion-deletion mutations (indels) were detected in an average of 40% of sequences by CRISPResso analysis[20] (Figure 1D and 1E; Figure S1F), and reduced PDX1 protein levels (Figure 1F; Figures S2A and S2B) were detected. After CRISPR/Cas9 targeting of *PDX1*, qRT-PCR revealed ~60% reduction of mRNA encoding PDX1 (Figure 1G). In addition, we observed a trend of reduced total Insulin protein levels, similarly to our prior findings[12] using lentiviral-based CRISPR (Figure 1H). By contrast, we did not detect changes in GLUCAGON mRNA by qRT-PCR (Figure 1G) or protein by immunostaining and morphometry (Figures S3A and S3B). These results motivated studies to explore the potential of this CRISPR/Cas9 RNP approach to target non-coding DNA elements in primary human islet cells.

Targeting of candidate *cis*-regulatory genomic regions in human islet cells

We have used lentiCRISPR to identify native human β cell enhancer elements regulating *SIX2* and *SIX3*,[12] but it is unknown whether CRISPR/Cas9 RNP strategies can be used similarly. To assess this, we adapted CRISPR/Cas9 RNP-based methods to induce a deletion in a putative *cis*-regulatory element in human islets and to identify the effector transcripts. We investigated a putative regulatory element in the intronic region of *PITPNM2* linked by chromatin looping studies to *MPHOSPH9*, *PITPNM2*, and *C12orf65*[8] (Figure 2A; Figure S4). We electroporated dispersed islet cells with CRISPR/Cas9 RNP complexes with two sgRNAs (sg1 and sg2) to target DNA encompassing this postulated regulatory element (Figure 2A) and visualized Cas9-GFP fluorescence one day after electroporation (Figure 2B). Controls included CRISPR/Cas9 RNP complexes with a non-targeting sgRNA. Following reaggregation and pseudoislet culture, deep sequencing and CRISPResso analysis[20] of the indexed targeted amplicons detected indels and deletion efficiencies of >40% (Figures 2C and 2D). Sequencing analysis of the likeliest genomic off-target sites (STAR methods) revealed that indels were undetectable in 5/5 of these sites (Figures S5A–S5C). qRT-PCR revealed a significant reduction of *MPHOSPH9* mRNA while mRNAs encoding PITPNM2, C12orf65, or the nearby *ABCB9* gene were unaltered (Figure 2E).

Unexpectedly, *INS* mRNA levels were also reduced after CRISPR/Cas9 RNP targeting (Figure 2E). While total Insulin content did not change, we observed impaired glucose-stimulated Insulin secretion after CRISPR/Cas9 RNP targeting (Figures 2F and 2G). Thus, our studies provide *in vivo* evidence that this enhancer is active in native β cells, and that its activity impacts the expression of *MPHOSPH9* but not of other neighboring genes. Moreover, reduced *MPHOSPH9* expression was linked to impaired *INS* expression and glucose-stimulated Insulin secretion. *MPHOSPH9* encodes MPP9, a protein required for formation of primary cilia,[22] organelles known to govern hormone secretion by islet α and β cells.[23,24]

Multiplexed CRISPR/Cas9 RNP targeting of regulatory regions in human islet cells

Next, we investigated use of CRISPR/Cas9 RNP for multiplex targeting of *cis*-regulatory elements in human islet cells. *PCSK1* encodes for Prohormone Convertase 1/3 (PC1/3), an endopeptidase regulating processing of Proinsulin (Figure 3A), and linked by prior genome-wide association studies (GWASs) to human diabetes and obesity risk.[25,26] To target the established promoter and enhancer regulatory elements of *PCSK1* in native β cells (Figure S6A), we electroporated primary human islets with CRISPR/Cas9 RNP complexes encoding Cas9-GFP and two sgRNAs to induce a deletion of *PCSK1* promoter (*PCSK1*-Prom) or enhancer sequences (*PCSK1*-Enh; Figures 3A and 3B). Non-targeting sgRNAs complexed with Cas9-GFP served as controls. After electroporation and pseudoislet *in vitro* culture, we performed high-throughput sequencing (Mi-seq) of the targeted *PCSK1*-Prom (Figure 3D) and *PCSK1*-Enh amplicons (Figure 3E) and used CRISPResso analysis to quantify the degree and specificity of gene editing. With *PCSK1*-Prom sgRNAs (sg1 and sg2), we observed >90% of *PCSK1* promoter sequences were modified; by contrast, *PCSK1*-Enh sequences were not edited (Figure 3D). Similarly, >85% of enhancer sequences were modified using *PCSK1*-Enh1 sgRNAs (sg3 and sg4), while *PCSK1* promoter sequences were not altered (Figure 3E). Potential genomic off-target sites

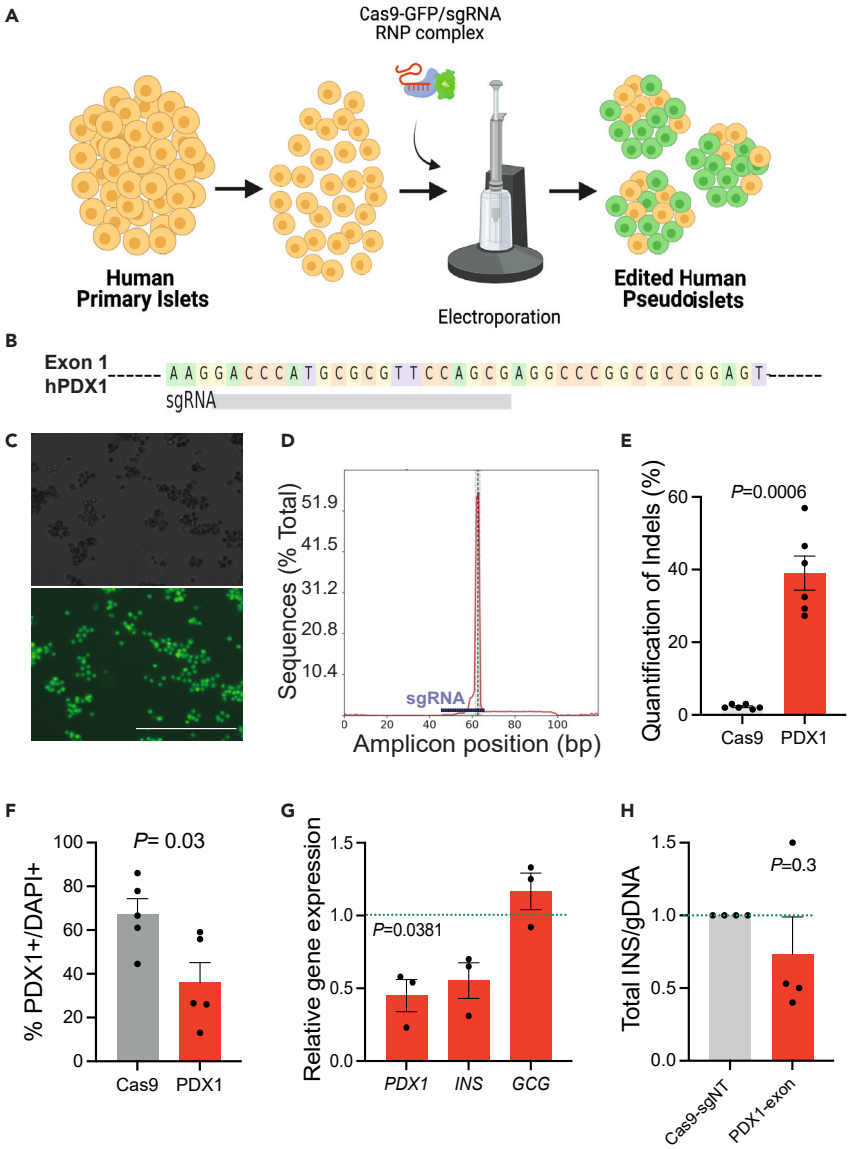

Figure 1. Efficient CRISPR/Cas9 RNP-mediated targeting of PDX1 in primary human islet cells

(A) Schematic of the human pseudoislet electroporation system with CRISPR/Cas9 RNP complexes.

(B) Fragment of human *PDX1* exon 1 sequence, showing the sgRNA sequence in gray.

(C) Human pseudoislets 1 day post-electroporation with Cas9-EGFP RNP and PDX1 sgRNAs complexes (top panel: bright field; bottom panel: blue light, 488 nm, scale bar: 500 μm).

(D) Quantification of editing frequency mapped to the reference amplicon using CRISPResso analysis. As expected, the mutations cluster around the predicted cleavage position based on the sgRNA sequence (expected cleavage site indicated by a vertical dotted line; sgRNA sequence: violet line).

(E) Quantification of indels after CRISPR/Cas9 RNP targeting of PDX1 (PDX1, red) or using a control sgRNA sequence (Cas9, gray) (n = 6 independent human islet donors).

(F) Total PDX1^{+} nuclei scored relative to total cells (DAPI+) counted from immunostaining. See also Figure S2 (n = 3 independent donor samples).

(G) qRT-PCR of pseudoislets, CRISPR-PDX1 (red), normalized to the CRISPR-Control (n = 3 independent donors).

(H) Total Insulin content of CRISPR/Cas9 electroporated cells normalized to genomic DNA (gDNA) content (n = 4 independent donor samples).

Data are presented as mean values ±SE. Two-tailed t tests were used to generate p values. See also Figures S1–S3.

were also sequenced (STAR methods), and no indels were detected in 6/6 of these sites (Figure S8). Thus, CRISPR/Cas9 RNP complexes were effective for independently targeting *PCSK1* promoter and enhancer elements.

In human islets, combinatorial targeting of independent regulatory elements could allow molecular studies of polygenic diabetes risk. For dual targeting of *PCSK1*-Prom and *PCSK1*-Enh, we used sgRNAs to induce a deletion in both the promoter and enhancer elements

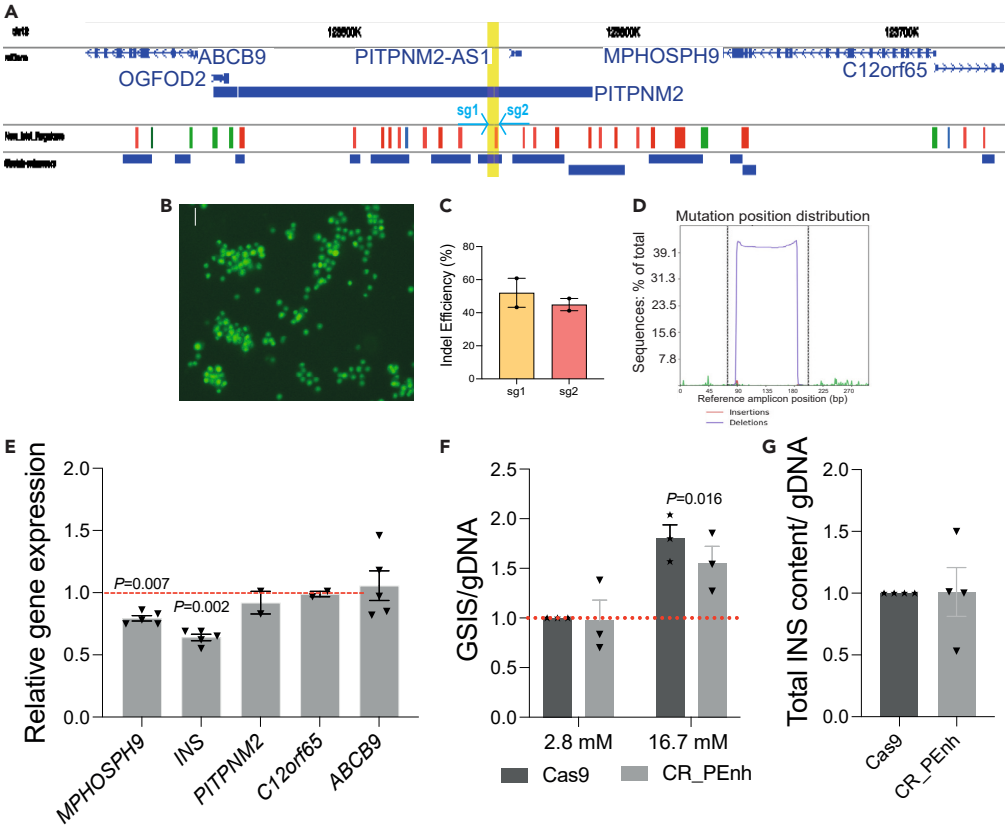

Figure 2. Linking candidate *cis*-regulatory genomic regions to their target genes in human islet cells

(A) Genome browser tracks[21] of the *MPHOSPH9* loci, highlighting in yellow a candidate *cis*-regulatory genomic region within the *PITPNM2* gene, and linked by pC-HiC to *PITPNM2*, *MPHOSPH9*, and *C12orf16*. See also Figure S4. The predicted enhancer (red, yellow highlight) was targeted with two sgRNAs (sg1 and sg2, turquoise arrows) designed to delete this element.

(B) Human islet cells expressing GFP one day following electroporation with the CRISPR/Cas9 RNP complexes.

(C) Quantification of editing frequency by each sg RNA mapped to the reference amplicon using CRISPResso analysis.[20] See also Figure S5.

(D) Histogram showing deletion of the region in between the two sgRNAs, generated with CRISPResso.

(E) RT-qPCR showing reduced expression of *MSPHOSPH9* and *INS*, but not *PITPNM2*, *c12orf65*, and *ABCC9* after deletion of the putative enhancer site with CR_PEnh compared to the Cas9 control.

(F) Glucose-Stimulated Insulin secretion for the control (Cas9) versus CR_PEnh groups.

(G) Total Insulin content for the Cas9 control versus CR_PEnh groups.

Data are presented as mean values ±SE. Two-tailed t tests were used to generate p values. **p < 0.05, ***p < 0.01.

(*PCSK1*-Prom+Enh; Figures 3A and 3B), separated by 28 kilobases. Both the *PCSK1*-Prom and *PCSK1*-Enh sequences were modified at similar levels (>80%) compared to targeting *PCSK1*-Prom or *PCSK1*-Enh regions alone (Figures 3D and 3E, Figures S7A–S7H). Thus, CRISPR/Cas9 RNP targeting induced simultaneous deletions of two distinct *PCSK1* regulatory elements. We did not detect genomic off-target indels at any of the six potential sites after the dual targeting (STAR methods; Figure S8). We also performed indexed PCRs of three independent amplicons within the 28 kB region between the targeted enhancer and promoter (internal amplicons 1, 2, and 3), as well as a "reference" amplicon located outside the targeted region (Figure S9A). Following Mi-seq sequencing, we quantified and calculated the ratios of internal/reference amplicons and did not detect significant differences between the control and *PCSK1*-Prom+Enh (Figure S9B). We also measured internal/reference amplicon ratios for two of these amplicons and islets targeted with *PCSK1*-Prom and *PCSK1*-Enh (Figures S9C and S9D). As expected, the targeting of only one of the regulatory elements did not result in large deletions. Finally, we also performed PCR of the genomic region connecting enhancer and promoter and confirmed that deletions spanning this region occurred in <20% of sequences after dual targeting (Figures S10A–S10D).

PCSK1 expression is regulated by glucose,[8] and we noted increased *PCSK1* mRNA levels in islet cells cultured in 16.7 mM glucose ("high") compared to those in 2.8 mM glucose ("basal"; Figure 3C), corroborating prior reports. To assess the role of the *PCSK1*-Prom and *PCSK1*-Enh elements in glucose-dependent *PCSK1* expression, we targeted *PCSK1*-Prom, *PCSK1*-Enh, or *PCSK1*-Prom+Enh and then measured *PCSK1* mRNA levels in pseudoislets at 2.8 mM or 16.7 mM glucose (Figure 3B and 3F–3H). As expected, cells electroporated with control Cas9-sgNT had increased *PCSK1* mRNA when cultured in high glucose compared to culture in basal glucose (Figures 3F–3H). However, *PCSK1* mRNA

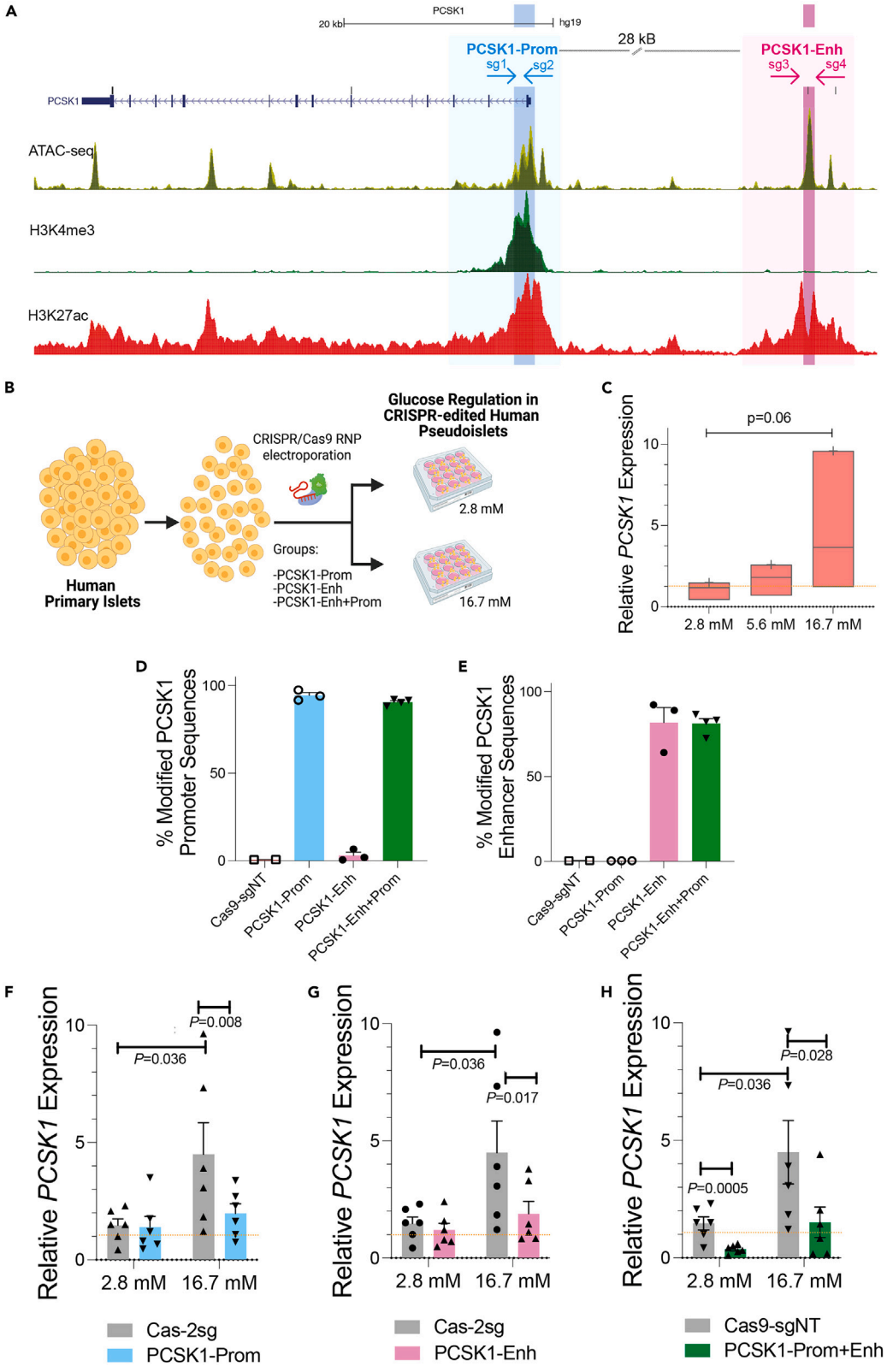
A
PCSK1
20 kb
hg19
28 kB
PCSK1-Prom
sg1
sg2
PCSK1-Enh
sg3
sg4
PCSK1
ATAC-seq
H3K4me3
H3K27ac
B
Glucose Regulation in CRISPR-edited Human Pseudoislets
CRISPR/Cas9 RNP electroporation
Human Primary Islets
Groups:
-PCSK1-Prom
-PCSK1-Enh
-PCSK1-Enh+Prom
2.8 mM
16.7 mM
C
p=0.06
Relative PCSK1 Expression
2.8 mM
5.6 mM
16.7 mM
D
% Modified PCSK1 Promoter Sequences
Cas9-sgNT
PCSK1-Prom
PCSK1-Enh
PCSK1-Enh+Prom
E
% Modified PCSK1 Enhancer Sequences
F
P=0.008
P=0.036
Relative PCSK1 Expression
2.8 mM
16.7 mM
Cas-2sg
PCSK1-Prom
G
P=0.036
P=0.017
Cas-2sg
PCSK1-Enh
H
P=0.028
P=0.036
P=0.0005
Cas9-sgNT
PCSK1-Prom+Enh

Figure 3. CRISPR/Cas9 RNP electroporation in human islet cells allows multiplex targeting of regulatory regions

(A) Genome browser tracks of *PCSK1* and its regulatory elements: *PCSK1* Promoter (*PCSK1*-Prom) and *PCSK1* Enhancer (*PCSK1*-Enh). Regulatory regions that show glucose-induced H3K27ac accessibility are highlighted: *PCSK1*-Prom (light blue, sg1 and sg2 are designed to induce a deletion of the turquoise region) and *PCSK1*-Enh (light pink, sg3 and sg4 are designed to induce a deletion of the dark pink region). Accessible chromatin regions in the human islets are shown by ATAC-seq, H3K4me3, and H3K27ac ChIP-seq. See also Figure S6.

(B) Schematics of the human pseudoislet CRISPR/Cas9 electroporation approach used for targeting of *PCSK1*-Prom and *PCSK1*-Enh, or simultaneous targeting of *PCSK1*-Prom+Enh, followed by culture at either basal (2.8 mM) or high (16.7 mM) glucose concentrations.

(C) qRT-PCR of *PCSK1* in pseudoislets at 2.8, 5.6, and 16.7 mM glucose (n = 3 independent donors).

(D and E) CRISPResso[20] quantification of editing efficiency on (D) *PCSK1* Promoter sequence and (E) *PCSK1* enhancer sequence, after targeting with CRISPR/Cas9 control (Cas9-sgNT), *PCSK1*-Prom, *PCSK1*-Enh, or *PCSK1*-Enh+Prom (n = 3 independent donors for *PCSK1*-Enh and *PCSK1*-Prom and n = 4 for *PCSK1*-Enh+Prom. See also Figures S7–S10.

(F–H) Measurements of *PCSK1* expression 5 days after CRISPR/Cas9 RNP targeting of (F) *PCSK1*-Prom, (G) *PCSK1*-Enh, and (H) *PCSK1*-Enh+Prom compared to a control (Cas9-2sg) in human pseudoislets and culture at 2.8 mM versus 16.7 mM glucose (n = 5 independent donors). Data are presented as mean values ±SE. Two-tailed t tests were used to generate p values.

induction was blunted after targeting *PCSK1*-Prom, *PCSK1*-Enh, or *PCSK1*-Prom+Enh (Figures 3F–3H). Additionally, at low glucose concentration, *PCSK1* mRNA was reduced after targeting of *PCSK1*-Prom+Enh but not in cells with *PCSK1*-Prom or *PCSK1*-Enh targeting alone (Figure 3H: $p < 0.05$). These studies therefore reveal an additive requirement for both *PCSK1*-Prom and *PCSK1*-Enh in regulating *PCSK1* expression in basal glucose conditions.

We next evaluated roles of the *PCSK1*-Prom and *PCSK1*-Enh elements in glucose-dependent *PCSK1* expression in islet cells cultured in normoglycemic conditions (5.6 mM). In this case, we also observed reduced *PCSK1* mRNA after individual targeting of *PCSK1*-Prom or *PCSK1*-Enh or after dual *PCSK1*-Prom+Enh (Figure 4A). Levels of mRNAs encoding PCSK2 and GLUCAGON did not change following CRISPR targeting of *PCSK1* regulatory elements in cells cultured at 5.6 mM glucose concentration (Figures 4A and 4B), 2.8 mM, or 16.7 mM glucose (Figure S11C). Glucose-dependent regulation of *INS* or *IAPP* (Figures 4C and 4D; Figures S11A and S11B) was also unaffected. Likewise, levels of mRNAs encoding *ELL2* and *CAST*, two genes neighboring *PCSK1* and located in the same topologically associated domain (TAD) as the *PCSK1*-Prom and *PCSK1*-Enh elements, were not altered (Figures 4E and 4F). Thus, we achieved CRISPR/Cas9 RNP-based targeting of two non-coding regulatory regions in human β-cells, and our *in vivo* studies revealed a selective, glucose-dependent impact on the expression of *PCSK1*.

Impaired Insulin processing and secretion after targeting *PCSK1* regulatory elements

To assess the impact of targeting *PCSK1* regulatory elements on β cell function, we measured processing and secretion of Proinsulin and Insulin (Figure 4G). After CRISPR/Cas9 RNP targeting of *PCSK1*-Prom, *PCSK1*-Enh, or *PCSK1*-Prom+Enh, we observed impaired Insulin secretion after stimulation with 16.7 mM glucose (Figure 4H). Moreover, challenge with 16.7 mM + the secretion potentiator IBMX revealed impaired Insulin secretion selectively after *PCSK1*-Prom+Enh targeting (Figure 4H), compared to targeting *PCSK1*-Prom or *PCSK1*-Enh alone. By contrast, Proinsulin secretion and total Insulin content in the *PCSK1*-Prom, *PCSK1*-Enh, or *PCSK1*-Prom+Enh groups were not significantly changed compared to controls (Figures 4I and 4J). However, total Proinsulin levels were significantly increased after CRISPR/Cas9 RNP targeting of *PCSK1*-Prom, *PCSK1*-Enh, and *PCSK1*-Prom+Enh, compared to the control (Figures 4K and 4L). Correspondingly, the average ratio of Insulin secretion/total Proinsulin trended to be reduced after targeting of *PCSK1* regulatory regions (Figure S11D). In sum, our studies with the CRISPR/Cas9 RNP approach suggest that the architecture and function of non-coding genomic regions can be interrogated in native human islet cells, including studies on gene regulation and β cell function after simultaneous targeting of distinct regulatory elements.

DISCUSSION

Here we report successful genome editing in primary human islets using CRISPR/Cas9 RNP complexed with sgRNAs, revealing functions of *cis*-regulatory elements in human β cells. In the sole prior report of CRISPR/Cas9 targeting in primary human islets, we showed that coding and non-coding DNA in adult, post-mitotic pancreatic islet cells can be edited using lentivirus-based delivery of sgRNA and Cas9 enzyme.[12] However, lentiviral transduction of dispersed human islet cells in that study was relatively inefficient, precluding multiplex targeting or other studies. Electroporation of Cas9 RNP complexes has been used for genome editing in primary human T cells and other dividing cell types.[15–17] However, adult human islet cells are post-mitotic, and it was unclear if Cas9 RNP delivery could achieve sufficient editing. Successful targeting of coding and non-coding DNA elements shown here should expand the uses of CRISPR for investigating human islet biology and islet-based diabetes risk.

Cas9 RNP complex electroporation efficiently targeted PDX1 coding sequence, and a postulated regulatory element previously linked by islet pc-HiC to *MPHOSPH9*, *PITPNM2*, and *C12orf65*.[8] Our CRISPR/Cas9 RNP targeting showed selective impaired expression of the *MPHOSPH9* gene. *MPHOSPH9* encodes a protein required for cilia formation, an organelle essential for β and α cell function.[23,24] Moreover, reduced expression of *MPHOSPH9* was accompanied by decreased *INS* mRNA levels and Insulin secretion. These findings highlight the potential for CRISPR/Cas9 RNP approaches to clarify the roles of *cis*-regulatory elements in islet gene regulation.

PCSK1 is expressed at a high "basal" level in human β cells and encodes PC1/3, an endopeptidase essential for Proinsulin processing. Glucose stimulates *PCSK1* expression, and prior studies demonstrated glucose-stimulated H3K27ac increases associated with the *PCSK1* promoter and a distal enhancer,[8] suggesting that these elements might regulate glucose-responsive *PCSK1* expression. In both T1D and

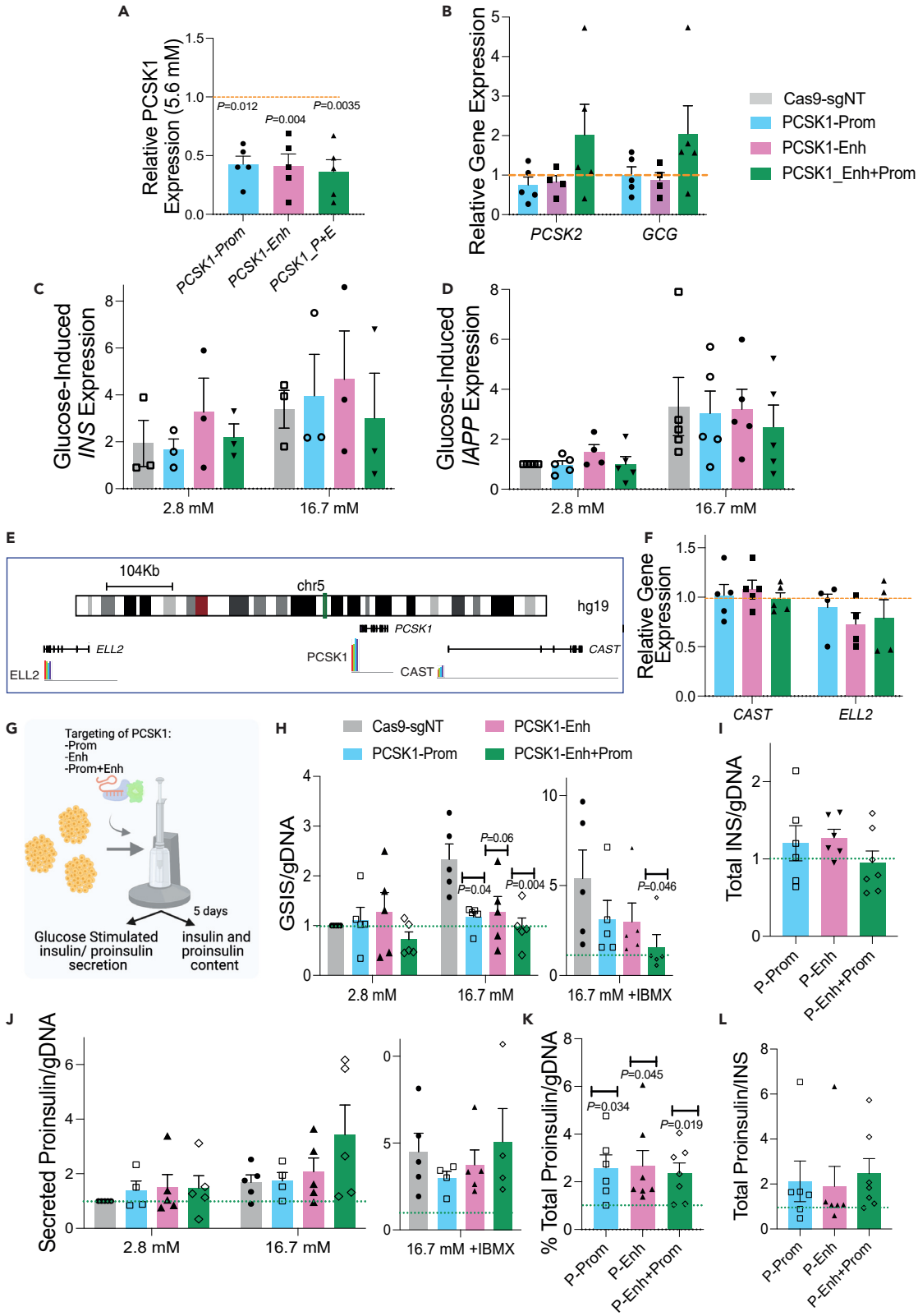
A
Relative PCSK1 Expression (5.6 mM)
P=0.012
P=0.004
P=0.0035
PCSK1-Prom
PCSK1-Enh
PCSK1_P+E
B
Relative Gene Expression
PCSK2
GCG
Cas9-sgNT
PCSK1-Prom
PCSK1-Enh
PCSK1_Enh+Prom
C
Glucose-Induced INS Expression
2.8 mM
16.7 mM
D
Glucose-Induced IAPP Expression
2.8 mM
16.7 mM
E
104Kb
chr5
hg19
PCSK1
ELL2
CAST
F
Relative Gene Expression
CAST
ELL2
G
Targeting of PCSK1:
-Prom
-Enh
-Prom+Enh
5 days
Glucose Stimulated insulin/ proinsulin secretion
insulin and proinsulin content
H
Cas9-sgNT
PCSK1-Prom
PCSK1-Enh
PCSK1-Enh+Prom
GSIS/gDNA
P=0.04
P=0.06
P=0.004
P=0.046
2.8 mM
16.7 mM
16.7 mM +IBMX
I
Total INS/gDNA
P-Prom
P-Enh
P-Enh+Prom
J
Secreted Proinsulin/gDNA
2.8 mM
16.7 mM
16.7 mM +IBMX
K
% Total Proinsulin/gDNA
P=0.034
P=0.045
P=0.019
P-Prom
P-Enh
P-Enh+Prom
L
Total Proinsulin/INS
P-Prom
P-Enh
P-Enh+Prom

Figure 4. Selective impairment of *PCSK1* expression and impaired Insulin processing and secretion following CRISPR/Cas9 RNP targeting of *PCSK1* regulatory elements

(A and B) RT-qPCR after CRISPR/Cas9 RNP targeting of *PCSK1*-Prom (turquoise), *PCSK1*-Enh (pink), or *PCSK1*-Enh+Prom (green): (A and B) Following culture at 5.6 mM glucose, and measurement of mRNA levels of (A) *PCSK1* and (B) *PCSK2* and *GCG* (n = 5 donors).

(C and D) Following culture at 2.8 mM versus 16.7 mM glucose and measurement of mRNA levels of glucose regulated (C) *INS* (n = 3) and (D) *IAPP* expression (n = 5).

(E) Scheme of the *PCSK1* locus, showing *PCSK1* neighboring genes.

(F) RT-qPCR of *CAST* and *ELL2* following CRISPR/Cas9 RNP targeting of *PCSK1* regulatory regions (n = 5 independent donors for *CAST* and n = 4 for *ELL2*). Data are presented as mean values ±SE. Two-tailed t tests were used to generate p values. *$p < 0.05$.

(G–L) (G) Scheme of electroporation of CRISPR/Cas9 RNP complexes with sgRNAs targeting *PCSK1*-Prom (turquoise bars), *PCSK1*-Enh (pink bars), *PCSK1*-Enh+Prom (green bar), or the control Cas9-sgNT followed by measurements of: (H) Glucose-stimulated Insulin Secretion (n = 5), (I) Total INS content (n = 5), (J) Glucose-stimulated Proinsulin Secretion (n = 4), (K) Total Proinsulin Content (n = 6–7), (L) Ratio of Proinsulin/Insulin (n = 6–7). See also Figure S11. Data are presented as mean values ±SE. Two-tailed t tests were used to generate p values. *$p < 0.05$, **$p < 0.005$.

T2D, PC1/3 activity appears reduced, and circulating Proinsulin:Insulin ratios are increased[27] (reviewed in Ramzy et al.[28]). These regulatory features motivated CRISPR targeting of these postulated *PCSK1 cis*-regulatory elements, including multiplexed targeting of promoter and enhancer. While we cannot fully rule out the occurrence of large deletions between the two targeted regulatory elements, two independent experiments indicate that such events might have occurred in <20% of the sequences. Moreover, our sequencing analysis did not reveal duplication or reversion events. Cas9 RNP has a relatively short half-life and does not become integrated into the genome, and this might reduce the frequency of such larger genomic rearrangements. Multiplexed targeting with Cas9 RNP revealed that basal *PCSK1* expression was reduced only when both promoter and enhancer were mutated. This also resulted in a trend toward increased expression of α-cell markers, such as GCG and PCSK2, likely reflecting expected variation of islet transcriptomes between donors. By contrast, CRISPR/Cas9 RNP targeting revealed that each element is required for glucose-induced *PCSK1* expression and impacts insulin secretion and total proinsulin levels. Overall, our approach revealed collaboration between *cis*-regulatory elements, a concept tested in other systems[16,29] but not previously investigated by gene targeting in primary human islet cells. Further application of this CRISPR/Cas9 RNP approach could be fruitful in dissecting the role of elements containing additional candidate diabetes risk SNPs, including identification of their genetic targets in human islet cells. Together with prior work,[12] our results also show that efficiency of the targeting is locus dependent. CRISPR-based editing efficiency can be enhanced by targeting proliferating cells[12]; further studies are needed to assess if mitogenic stimulation of adult human islet cells, which are largely post-mitotic, could enhance CRISPR/RNP targeting efficiency. In addition, future efforts should also be directed to explore additional gene-editing possibilities, such as engineered DNA-free virus-like particles (VLPs),[30] base editing,[31] and prime editing[32] strategies. One caveat of our studies is that we were unable to correlate phenotypes in single cells or clonal populations with gene editing. The non-dividing nature of adult human islet cells precludes the enrichment studies usually performed for cell lines. Approaches such as TARGET-seq[33] or other single cell-based approaches could be useful in future studies to assess gene-editing heterogeneity.

In summary, CRISPR/Cas9 RNP electroporation in primary human islets allowed (1) highly efficient targeting (deletion) of non-coding DNAs, (2) simultaneous deletion of two regulatory elements, and (3) functional assessment of regulatory impacts from multiplex targeting of non-coding DNA, including dynamic physiological regulation by glucose. These innovations advance the use of genome editing to dissect the genetic regulatory mechanisms in islets that underlie diabetes risk.

Limitations of the study

A main limitation of our study is that genome editing in primary non-dividing human islet cells—which are largely post-mitotic—results in a heterogeneous mixture of cells with various phenotypes, reflecting imprecise repair mechanisms at the targeted site. Also, despite high targeting efficiencies, not every cell is edited in the final population. Future studies will need to purify edited cells to correlate phenotypes in single cells with specific gene editing. Despite these caveats, the efficiency of gene disruption is sufficiently high to allow linkage of specific, edited genotypes to phenotypes, including the impact of editing non-coding DNA elements on gene expression. When performing multiplexed targeting of two postulated gene regulatory elements, we used interspersed genomic PCR to estimate that the frequency of deletions spanning the two elements was less than 20%; whole-genome sequencing experiments, beyond the scope of this study, would be required to quantify the actual percentage of such large deletions.

STAR★METHODS

Detailed methods are provided in the online version of this paper and include the following:

- KEY RESOURCES TABLE
- RESOURCE AVAILABILITY
  - Lead contact
  - Materials availability
  - Data and code availability
- METHOD DETAILS

- CRISPR/Cas9 RNP complexes assembly
- Human pseudoislet generation and CRISPR/Cas9 RNP complexes electroporation
- Live/dead staining and fluorescent-activated cell flow of human islet cells
- Genomic DNA extraction, Mi-Seq sequencing, and CRISPResso analysis
- Evaluation of CRISPR/Cas9 off-target effects and PCRs to detect large deletions
- Immunohistochemistry of CRISPR/Cas9 RNP complexes
- RNA extraction and quantitative RT-PCR
- Glucose-stimulated human insulin and proinsulin secretion, insulin, and proinsulin content measurement
- Data visualization

- QUANTIFICATION AND STATISTICAL ANALYSIS

SUPPLEMENTAL INFORMATION

Supplemental information can be found online at https://doi.org/10.1016/j.isci.2023.108693.

ACKNOWLEDGMENTS

We thank past and current members of the Kim group, especially S. Park, for technical advice and support. We thank Dr. Jocelyn Manning Fox, Mrs. Nancy Smith, and Mr. James Lyon (University of Alberta) for their contributions to human islet isolations. We gratefully acknowledge organ donors and their families, Canadian organ procurement organizations, particularly the Human Organ Procurement and Exchange (HOPE) program and the Trillium Gift of Life Network, and islet procurement through the Alberta Diabetes Institute Islet Core, Integrated Islet Distribution Program (U.S. NIH UC4DK098085), the National Disease Research Interchange, and the International Institute for the Advancement of Medicine. R.J.B. was supported by a postdoctoral fellowship from JDRF (3-PDF-2018-584-A-N). A.L.G. is supported by a Wellcome Senior Fellowship (200837/Z/16/Z) and by NIDDK UM-1DK126185. Work in the Kim lab was supported by NIH awards (R01 DK107507; R01 DK108817; U01 DK123743 to S.K.K.) and JDRF Northern California Center of Excellence (to S.K.K. and A.M.). Work here was also supported by NIH grant P30 DK116074 (S.K.K.), the Stanford Islet Research Core, and Diabetes Genomics and Analysis Core of the Stanford Diabetes Research Center.

AUTHOR CONTRIBUTIONS

R.J.B. and S.K.K. conceptualized the study and guided the work. Methodology: R.J.B., A.L.G., S.K.K.; investigation: R.J.B., S.H.K., W.Z., A.M.; writing: R.J.B. and S.K.K. wrote the manuscript with input from all coauthors; visualization: R.J.B.; supervision: S.K.K.; funding acquisition: R.J.B., A.M., A.L.G., S.K.K.

DECLARATION OF INTERESTS

A.M. is a co-founder of Arsenal Biosciences, Function Bio, Spotlight Therapeutics, and Survey Genomics, serves on the boards of directors at Function Bio, Spotlight Therapeutics, and Survey Genomics, is a member of the scientific advisory boards of Arsenal Biosciences, Function Bio, Spotlight Therapeutics, Survey Genomics, NewLimit, Amgen, Tenaya, and Lightcast, owns stock in Arsenal Biosciences, Function Bio, Spotlight Therapeutics, NewLimit, Survey Genomics, Tenaya, and Lightcast, and has received fees from Arsenal Biosciences, Spotlight Therapeutics, NewLimit, 23andMe, PACT Pharma, Juno Therapeutics, Tenaya, Lightcast, Trizell, Vertex, Merck, Amgen, Genentech, AlphaSights, Rupert Case Management, Bernstein, GLG, ClearView Healthcare Partners, and ALDA. A.M. is an investor in and informal advisor to Offline Ventures and a client of EPIQ. The Marson laboratory has received research support from Juno Therapeutics, Epinomics, Sanofi, GlaxoSmithKline, Gilead, and Anthem. A.L.G.'s spouse holds stock options in Roche and is an employee of Genentech.

Received: June 26, 2023
Revised: October 27, 2023
Accepted: December 5, 2023
Published: December 8, 2023

REFERENCES

1. Ashcroft, F.M., and Rorsman, P. (2012). Diabetes mellitus and the β cell: the last ten years. Cell *148*, 1160–1171.
2. Gloyn, A.L., Pearson, E.R., Antcliff, J.F., Proks, P., Bruining, G.J., Slingerland, A.S., Howard, N., Srinivasan, S., Silva, J.M.C.L., Molnes, J., et al. (2004). Activating mutations in the gene encoding the ATP-sensitive potassium-channel subunit Kir6.2 and permanent neonatal diabetes. N. Engl. J. Med. *350*, 1838–1849.
3. Njølstad, P.R., Søvik, O., Cuesta-Muñoz, A., Bjørkhaug, L., Massa, O., Barbetti, F., Undlien, D.E., Shiota, C., Magnuson, M.A., Molven, A., et al. (2001). Neonatal diabetes mellitus due to complete glucokinase deficiency. N. Engl. J. Med. *344*, 1588–1592.
4. Stoffers, D.A., Zinkin, N.T., Stanojevic, V., Clarke, W.L., and Habener, J.F. (1997). Pancreatic agenesis attributable to a single nucleotide deletion in the human IPF1 gene coding sequence. Nat. Genet. *15*, 106–110.
5. Mahajan, A., Taliun, D., Thurner, M., Robertson, N.R., Torres, J.M., Rayner, N.W., Payne, A.J., Steinthorsdottir, V., Scott, R.A., Grarup, N., et al. (2018). Fine-mapping type 2 diabetes loci to single-variant resolution using high-density imputation and islet-specific epigenome maps. Nat. Genet. *50*, 1505–1513.
6. Viñuela, A., Varshney, A., van de Bunt, M., Prasad, R.B., Asplund, O., Bennett, A., Boehnke, M., Brown, A.A., Erdos, M.R.,

Fadista, J., et al. (2020). Genetic variant effects on gene expression in human pancreatic islets and their implications for T2D. Nat. Commun. *11*, 4912.

7. Alvarez-Dominguez, J.R., Donaghey, J., Rasouli, N., Kenty, J.H.R., Helman, A., Charlton, J., Straubhaar, J.R., Meissner, A., and Melton, D.A. (2020). Circadian Entrainment Triggers Maturation of Human In Vitro Islets. Cell Stem Cell *26*, 108–122.e10.
8. Miguel-Escalada, I., Bonàs-Guarch, S., Cebola, I., Ponsa-Cobas, J., Mendieta-Esteban, J., Atla, G., Javierre, B.M., Rolando, D.M.Y., Farabella, I., Morgan, C.C., et al. (2019). Human pancreatic islet three-dimensional chromatin architecture provides insights into the genetics of type 2 diabetes. Nat. Genet. *51*, 1137–1148.
9. Benaglio, P., Zhu, H., Okino, M.L., Yan, J., Elgamal, R., Nariai, N., Beebe, E., Korgaonkar, K., Qiu, Y., Donovan, M.K.R., et al. (2022). Type 1 diabetes risk genes mediate pancreatic beta cell survival in response to proinflammatory cytokines. Cell Genom. *2*, 100214.
10. Cebola, I. (2019). Pancreatic Islet Transcriptional Enhancers and Diabetes. Curr. Diab. Rep. *19*, 145.
11. Claringbould, A., and Zaugg, J.B. (2021). Enhancers in disease: molecular basis and emerging treatment strategies. Trends Mol. Med. *27*, 1060–1073.
12. Bevacqua, R.J., Dai, X., Lam, J.Y., Gu, X., Friedlander, M.S.H., Tellez, K., Miguel-Escalada, I., Bonàs-Guarch, S., Atla, G., Zhao, W., et al. (2021). CRISPR-based genome editing in primary human pancreatic islet cells. Nat. Commun. *12*, 2397.
13. Friedlander, M.S.H., Nguyen, V.M., Kim, S.K., and Bevacqua, R.J. (2021). Pancreatic Pseudoislets: An Organoid Archetype for Metabolism Research. Diabetes *70*, 1051–1060.
14. D'Astolfo, D.S., Pagliero, R.J., Pras, A., Karthaus, W.R., Clevers, H., Prasad, V., Lebbink, R.J., Rehmann, H., and Geijsen, N. (2015). Efficient intracellular delivery of native proteins. Cell *161*, 674–690.
15. Schumann, K., Lin, S., Boyer, E., Simeonov, D.R., Subramaniam, M., Gate, R.E., Haliburton, G.E., Ye, C.J., Bluestone, J.A., Doudna, J.A., and Marson, A. (2015). Generation of knock-in primary human T cells using Cas9 ribonucleoproteins. Proc. Natl. Acad. Sci. USA *112*, 10437–10442.
16. Hultquist, J.F., Schumann, K., Woo, J.M., Manganaro, L., McGregor, M.J., Doudna, J., Simon, V., Krogan, N.J., and Marson, A. (2016). A Cas9 Ribonucleoprotein Platform for Functional Genetic Studies of HIV-Host Interactions in Primary Human T Cells. Cell Rep. *17*, 1438–1452.
17. Schumann, K., Raju, S.S., Lauber, M., Kolb, S., Shifrut, E., Cortez, J.T., Skartsis, N., Nguyen, V.Q., Woo, J.M., Roth, T.L., et al. (2020). Functional CRISPR dissection of gene networks controlling human regulatory T cell identity. Nat. Immunol. *21*, 1456–1466.
18. Lattanzi, A., Meneghini, V., Pavani, G., Amor, F., Ramadier, S., Felix, T., Antoniani, C., Masson, C., Alibeu, O., Lee, C., et al. (2019). Optimization of CRISPR/Cas9 Delivery to Human Hematopoietic Stem and Progenitor Cells for Therapeutic Genomic Rearrangements. Mol. Ther. *27*, 137–150.
19. Chandrasekaran, A.P., Song, M., Kim, K.S., and Ramakrishna, S. (2018). Different Methods of Delivering CRISPR/Cas9 Into Cells. Prog. Mol. Biol. Transl. Sci. *159*, 157–176.
20. Pinello, L., Canver, M.C., Hoban, M.D., Orkin, S.H., Kohn, D.B., Bauer, D.E., and Yuan, G.C. (2016). Analyzing CRISPR genome-editing experiments with CRISPResso. Nat. Biotechnol. *34*, 695–697.
21. Mularoni, L., Ramos-Rodríguez, M., and Pasquali, L. (2017). The Pancreatic Islet Regulome Browser. Front. Genet. *8*, 13.
22. Huang, N., Zhang, D., Li, F., Chai, P., Wang, S., Teng, J., and Chen, J. (2018). M-Phase Phosphoprotein 9 regulates ciliogenesis by modulating CP110-CEP97 complex localization at the mother centriole. Nat. Commun. *9*, 4511.
23. Wu, C.T., Hilgendorf, K.I., Bevacqua, R.J., Hang, Y., Demeter, J., Kim, S.K., and Jackson, P.K. (2021). Discovery of ciliary G protein-coupled receptors regulating pancreatic islet insulin and glucagon secretion. Genes Dev. *35*, 1243–1255.
24. Hughes, J.W., Cho, J.H., Conway, H.E., DiGruccio, M.R., Ng, X.W., Roseman, H.F., Abreu, D., Urano, F., and Piston, D.W. (2020). Primary cilia control glucose homeostasis via islet paracrine interactions. Proc. Natl. Acad. Sci. USA *117*, 8912–8923.
25. Stijnen, P., Tuand, K., Varga, T.V., Franks, P.W., Aertgeerts, B., and Creemers, J.W.M. (2014). The association of common variants in PCSK1 with obesity: a HuGE review and meta-analysis. Am. J. Epidemiol. *180*, 1051–1065.
26. Nead, K.T., Li, A., Wehner, M.R., Neupane, B., Gustafsson, S., Butterworth, A., Engert, J.C., Davis, A.D., Hegele, R.A., Miller, R., et al. (2015). Contribution of common non-synonymous variants in PCSK1 to body mass index variation and risk of obesity: a systematic review and meta-analysis with evidence from up to 331 175 individuals. Hum. Mol. Genet. *24*, 3582–3594.
27. Wasserfall, C., Nick, H.S., Campbell-Thompson, M., Beachy, D., Haataja, L., Kusmartseva, I., Posgai, A., Beery, M., Rhodes, C., Bonifacio, E., et al. (2017). Persistence of Pancreatic Insulin mRNA Expression and Proinsulin Protein in Type 1 Diabetes Pancreata. Cell Metab. *26*, 568–575.e3.
28. Ramzy, A., and Kieffer, T.J. (2022). Altered islet prohormone processing: a cause or consequence of diabetes? Physiol. Rev. *102*, 155–208.
29. McCarty, N.S., Graham, A.E., Studená, L., and Ledesma-Amaro, R. (2020). Multiplexed CRISPR technologies for gene editing and transcriptional regulation. Nat. Commun. *11*, 1281.
30. Raguram, A., Banskota, S., and Liu, D.R. (2022). Therapeutic in vivo delivery of gene editing agents. Cell *185*, 2806–2827.
31. Anzalone, A.V., Randolph, P.B., Davis, J.R., Sousa, A.A., Koblan, L.W., Levy, J.M., Chen, P.J., Wilson, C., Newby, G.A., Raguram, A., and Liu, D.R. (2019). Search-and-replace genome editing without double-strand breaks or donor DNA. Nature *576*, 149–157.
32. Komor, A.C., Kim, Y.B., Packer, M.S., Zuris, J.A., and Liu, D.R. (2016). Programmable editing of a target base in genomic DNA without double-stranded DNA cleavage. Nature *533*, 420–424.
33. Rodriguez-Meira, A., O'Sullivan, J., Rahman, H., and Mead, A.J. (2020). TARGET-Seq: A Protocol for High-Sensitivity Single-Cell Mutational Analysis and Parallel RNA Sequencing. STAR Protoc. *1*, 100125.
34. Labun, K., Montague, T.G., Krause, M., Torres Cleuren, Y.N., Tjeldnes, H., and Valen, E. (2019). CHOPCHOP v3: expanding the CRISPR web toolbox beyond genome editing. Nucleic Acids Res. *47*, W171–W174.
35. Brinkman, E.K., Chen, T., Amendola, M., and van Steensel, B. (2014). Easy quantitative assessment of genome editing by sequence trace decomposition. Nucleic Acids Res. *42*, e168.

STAR★METHODS

KEY RESOURCES TABLE

REAGENT or RESOURCE	SOURCE	IDENTIFIER
Antibodies		
mouse anti-PDX1	BD	562160
Guinea pig anti-insulin	Dako	A0564
mouse anti-glucagon	Sigma	G2654
Alexa Fluor 555 Donkey anti Mouse Secondary Antibody	Invitrogen	A32773
Alexa Fluor® 647-AffiniPure Donkey Anti-Mouse IgG (H + L)	Jackson ImmunoResearch	715-605-150
Biological samples		
Refer to Table S1 for De-identified donor information.	IIDP	https://iidp.coh.org/
Refer to Table S1 for De-identified donor information.	ADI	https://www.ualberta.ca/alberta-diabetes/core-services/isletcore.html
Chemicals, peptides, and recombinant proteins		
Cas9, fused with enhanced GFP 3X NLS	Sigma-Aldrich	CAS9GFPPRO-250UG
Critical commercial assays		
Arcturus PicoPure RNA Isolation Kit	Life Technologies	KIT0204
Arcturus PicoPure DNA Isolation Kit	Life Technologies	KIT0103
Maxima First Strand cDNA synthesis kit	Thermo Scientific	K1642
Taqman Gene Expression Master Mix	Thermo Scientific	4369542
Human insulin ELISA kit	Mercodia	10-1132-01
Human proinsulin ELISA kit	Mercodia	10-1118-01
Oligonucleotides		
sgRNA sequences -Refer to Table S2.	Synthego	N/A
Primer sequences- Refer to Table S3.	IDTDNA	N/A
Software and algorithms		
CRISPResso	Pinello et al.[20]	N/A
CHOP-CHOP	Labun et al.[34]	N/A
TIDE analysis	Brinkman et al.[35]	N/A
FlowJo	https://www.flowjo.com/	N/A
Prism 6.0	GraphPad Software Inc., San Diego, CA	N/A
ImageJ	https://ImageJ.net/ij/	N/A
Other		
Electroporator NeonTM	Thermo Fisher Scientific	NEON1
Neon™ Transfection System 10 µL Kit	Thermo Fisher Scientific	MPK1025

RESOURCE AVAILABILITY

Lead contact

Further information and requests for resources and reagents should be directed to and will be fulfilled by the lead contact, Seung K Kim (seungkim@stanford.edu).

Materials availability

This study did not generate new unique reagents.

Data and code availability

(1) Data reported in this paper will be shared by the lead contact upon request.
(2) This paper does not report original code.
(3) Primary human islets were used for this study. Organs and islets were procured through the Integrated Islet Distribution Network (IIDP), National Diabetes Research Institute (NDRI) and the Alberta Diabetes Institute (ADI) Islet Core. De-identified human islets were obtained from healthy, non-diabetic organ donors with less than 18 h of cold ischemia time, and deceased due to acute trauma or anoxia. For this study, islets from 26 adult donors were used, and their sex, age and BMI are reported in Table S1.

METHOD DETAILS

CRISPR/Cas9 RNP complexes assembly

Cas9 from Streptococcus pyogenes, fused with enhanced GFP, recombinant, expressed in E. coli, 3X NLS was purchased from Sigma-Aldrich (CAS9GFPPRO). The sgRNAs used in this study were designed using E-CRISPR and MIT CRISPR design tool. Chemically modified sgRNAs (with 2′-O-Methyl at 3 first and last bases, and 3′ phosphorothiate bonds between first 3 and last 2 bases) were purchased from Synthego. For CRISPR/Cas9 RNP complexes assembly, Cas9GFPPRO was complexed to sgRNAs and incubated at room temperature for 15 min. For 1X concentration, 1250 ng Cas9GFPPRO were incubated with 7.5 pg sgRNAs in 5 μl buffer R (NeonTM, Thermo Fisher Scientific). For 2X condition, double concentration was used (Figure S1A). The sgRNA sequences used in this study can be found in Table S2.

Human pseudoislet generation and CRISPR/Cas9 RNP complexes electroporation

Human islets were dispersed into a single cell suspension by enzymatic digestion (Accumax, Invitrogen). For each electroporation pulse with 10 μl tips of the NeonTM transfection system (Thermo Fisher Scientific), 150,000 cells were resuspended in 5 μl buffer R. Following CRISPR/Cas9 RNP assembly, CRISPR/Cas9 RNP complexes were added to cells in buffer R. Electroporation conditions tested in Figure S1A consisted of: V1 = 1100V, 1 pulse, 40 ms, V2 = 1500 V, 3 pulses, 10 ms, V3 = 1600 V, 3 pulses, 10 ms. V3 was used for following experiments. Immediately after the pulse, cells were transferred into 24 well plates in culture medium comprised of RPMI 1640 (Gibco), 2.25 g/dL glucose, 1% penicillin/streptomycin (v/v, Gibco), and 2% human serum (Sigma-Aldrich). Electroporated islet cells were cultured in an Orbi-Shaker (34–206, Genesee Scientific) until day 5 or 6 prior to further molecular or physiological analysis. One day following electroporation, GFP expression was evaluated.

Live/dead staining and fluorescent-activated cell flow of human islet cells

Pseudoislets were dispersed into single cells -as detailed before-, resuspended in PBS and stained with LIVE/DEAD Fixable Near-IR dead cell stain kit (Life Technologies) for 30 min in the dark. A negative, unstained control was included. Labeled cells were run on an Aurora CS FACS using appropriate compensation controls and doublet removal. Quantification of Live/Dead cells was performed using FlowJo.

Genomic DNA extraction, Mi-Seq sequencing, and CRISPResso analysis

1000–5000 electroporated cells were used for genomic DNA (gDNA) extraction using the Arcturus PicoPure DNA Extraction Kit (Thermo Fisher Scientific) per the manufacturer's instructions. Next, extracted gDNA was amplified using the REPLI-g-mini Kit (Qiagen). 2 μl of extracted and amplified gDNA was used for nested PCR using Phusion U Green Multiplex PCR Master Mix (2X) (Thermo Scientific). PCR1 was performed with amplicon specific and barcode tail primers, with conditions consisting of initial 98 °C for 2 min, followed by 30 cycles, each composed of a denaturing step at 98 °C for 10 s, an annealing step at 61 °C for 20 s, and an extension step at 72 °C for 30 s, followed by a final extension at 72 °C for 2 min. PCR2 was included to add barcodes for sequencing, using publicly available Illumina Adapter sequences. Conditions consisted of initial 98 °C for 2 min, followed by 12 cycles, each composed of a denaturing step at 98 °C for 10 s, an annealing step at 61 °C for 20 s, and an extension step at 72 °C for 30 s, followed by a final extension at 72 °C for 2 min. PCR2 products were gel purified, using Zymoclean Gel DNA recovery kit (Zymo Research). Amplicon concentrations were measured using Qubit dsDNA HS (Thermo Fisher Scientific) and pooled for Miseq sequencing at 2 × 300 bp (Illumina, Stanford Functional Genomics Facility). CRISPResso analysis was performed of the sequenced amplicons, following the software pipeline designed by the Pinello Lab.[20] Primer sequences are summarized in Table S3.

Evaluation of CRISPR/Cas9 off-target effects and PCRs to detect large deletions

Off-target site prediction was performed using the CHOP-CHOP tool.[34] The potential off-target sites found had at least 2 mismatches with respect to the sgRNA sequence. PCR primers encompassing 3 of these potential off-target sites for each sgRNA were designed and the PCR amplicons were purified and sequenced. PCR was performed with Phusion U Green Multiplex PCR Master Mix (2X) (Thermo Scientific) in 35 cycles, each cycle composed of a denaturing step at 95°C for 1 min, an annealing step at 61°C for 30 s and an extension step at 68°C for 1 min, followed by final extension at 72°C for 5 min. Primer sequences are summarized in Table S3. Following sequencing, we performed TIDE[35] analyses to assess indel occurrence at these off target sites.

To assess occurrence of deletions of the region in between the targeted PCSK1 enhancer and promoter, we performed nested indexed amplification of 4 amplicons (three within the potentially deleted region -intPCR1, intPCR2 and intPCR3-and one reference amplicon, located

outside the presumably deleted region, Figure S9A). PCR1 and PCR2 were performed with Phusion U Green Multiplex PCR Master Mix (2X) (Thermo Scientific), gel purified, Miseq sequenced and CRISPResso analyzed as described above. The proportion of internal PCR amplicons/reference amplicon were calculated both for the control and *PCSK1*_Prom+Enh targeted groups. Primer sequences are included in Table S3.

To directly measure amplicons generated by deletion of the entire region in between the targeted promoter and enhancer, we performed multiplexed PCR, design shown in Figure S10A. Multiplex PCR was performed with Phusion U Green Multiplex PCR Master Mix (2X) (Thermo Scientific) in 30 cycles, each cycle composed of a denaturing step at 95°C for 1 min, an annealing step at 65°C for 20 s and an extension step at 72°C for 15 s, followed by a final extension at 72°C for 5 min. Primer sequences are summarized in Table S3. PCR products were run on a 1.5% low melt agarose gel for 40 minutes under a fixed voltage of 110 Volts. The gel was imaged using Axygen, gel documentation systems (Corning). Quantitation was performed via FIJI (ImageJ). A selection box with a fixed area was generated and utilized to report the mean intensity and area under the curve for all PCR products per condition. The background was subtracted for each lane, and the quantitation was normalized according to the product's size (bp).

Immunohistochemistry of CRISPR/Cas9 RNP complexes

For immunostaining, human pseudoislets were fixed for 1 h at 4°C and embedded in collagen (Wako Chemicals). Ten micrometers thick frozen sections were cut and stained following standard cryostaining protocols. Briefly, sections were washed in PBS, incubated with blocking solution followed by incubation in permeabilization/blocking buffer (1% bovine serum albumin, 0.2% non-fat milk, 0.5% Triton-X in PBS) for 1 h. Primary antibodies were mixed with permeabilization/blocking buffer and incubated at 4°C overnight. The following primary antibodies were used: mouse anti-PDX1, (BD 562160), Guinea pig anti-insulin (a0564 Dako), mouse anti-glucagon (G2654 Sigma), Alexa Fluor 555 Donkey anti Mouse Secondary Antibody (A32773; Invitrogen), Alexa Fluor 647-AffiniPure Donkey Anti-Mouse IgG (H + L) (715-605-150; Jackson ImmunoResearch). Slides were washed with PBS, incubated with secondary antibodies at room temperature for 2 h, and were preserved with mounting medium containing DAPI (Vector Labs, Vectashield H-1200). Images were obtained using a Zeiss Observer Z1 microscope. Total cell numbers, PDX1+ and INS+ cells were calculated using Analyze particle feature of ImageJ.

RNA extraction and quantitative RT-PCR

RNA was isolated from electroporated pseudoislet cells using the PicoPure RNA Isolation Kit (Life Technologies). cDNA was synthesized using the Maxima First Strand cDNA synthesis kit (Thermo Scientific) and gene expression was assessed by PCR using the Taqman Gene Expression Mix (Thermo Scientific). Data were analyzed using Prism 6.0 h (GraphPad Software Inc., San Diego, CA). Taqman probes used for this study are summarized in Table S3. Paired two-tailed t tests were used to indicate statistical significance, and data are presented as mean and standard deviation.

Glucose-stimulated human insulin and proinsulin secretion, insulin, and proinsulin content measurement

Glucose-Stimulated human insulin and proinsulin secretion were performed as batch assays on pseudoislets from CRISPR-Control and Cas9 targeted groups, with 30 pseudoislets as input, and supernatants were collected after 1 h incubation at 2.8 mM, 16.7 mM and 16.7 mM + IBMX glucose concentrations. To determine total cellular insulin or proinsulin content, pseudoislets were sonicated and lysed to extract the total cellular insulin or proinsulin content (Human insulin and proinsulin ELISA kits, Mercodia). gDNA from the same sonicated islets used for the insulin ELISAs was extracted and used for normalization.

Data visualization

Browser tracks were made with the UCSC genome browser. The graphics were made with BioRender.

QUANTIFICATION AND STATISTICAL ANALYSIS

For quantification of total cell numbers, PDX1+ and INS+ cells from immunostaining images, Analyze particle feature of ImageJ was used. Quantification of live/dead cells after flow, FlowJo was used. For measurement of total number of edited amplicons, CRISPResso was used.[34] Statistical analysis was performed using Prism 6.0 h (GraphPad Software Inc., San Diego, CA), normalizing to the CRISPR-Control and presented as mean with standard deviation. Paired two-tailed t tests were used to indicate statistical significance.